Inhomogeneous laser heating and phonon confinement in silicon nanowires: A micro-Raman scattering study

K. W. Adu,[1] H. R. Gutiérrez,[1] U. J. Kim,[1] and P. C. Eklund[1,2,*]
[1]*Department of Physics, Pennsylvania State University, University Park, Pennsylvania 16802, USA*
[2]*Department of Materials Science, The Pennsylvania State University, University Park, Pennsylvania 16802, USA*
(Received 12 May 2005; revised manuscript received 14 December 2005; published 27 April 2006)

Results of a systematic set of micro-Raman experiments on the changes in the line shape of the ~520 cm^{-1} one-phonon band in Si nanowires with laser flux Φ are presented. A complicated dependence of the 520 cm^{-1} Raman band asymmetry (A) with Φ is observed that depends *both* on the nanowire diameter *and* on the thermal anchoring of the wires to an indium foil substrate. With increasing power density in a ~1 μ focal spot common to micro-Raman spectroscopy, we see a clear growth in A that has nothing to do with phonon confinement. In fact, we can explain the complex changes in $A(\Phi)$ by extending the model [H. Richter, Z. P. Wang, and Y. Ley, Solid State Commun. **39**, 625 (1981)] to include an *inhomogeneous* heating in the Raman volume. The effects we observe in Si nanowires should be common to all semiconducting nanostructures and underscores the importance of demonstrating a flux-independent line shape when studying pure phonon confinement effects by Raman scattering.

DOI: 10.1103/PhysRevB.73.155333 PACS number(s): 78.67.Lt, 81.07.Bc, 78.66.Db, 81.07.Vb

INTRODUCTION

Small diameter crystalline semiconducting nanowires provide an interesting laboratory to study quantum confinement phenomena in quasi one-dimensional systems.[1,2] For example, their electronic states can be tuned via the wire diameter d, as the band gap should scale approximately as $1/d$ (Ref. 3). The phonon spectrum, or phonon dispersion, and how it depends on d, is no less important. At room temperature, for example, the phonons are expected to scatter the charge carriers. As the nanowire becomes smaller in diameter and becomes more "one dimensional," these "confined" phonons will be involved in dissipating the momentum in the charge carriers generated by the applied electric field. Therefore, a fundamental understanding of confined phonon states is essential to a complete understanding of charge and heat transport in *small diameter* nanowires.

So far, Raman scattering studies of phonon confinement in semiconducting nanowires have failed to produce a consistent prediction for the effective nanowire diameter at which phonon confinement becomes important. An asymmetry in the phonon Raman band(s) is predicted by the model of Richter, Wang and Ley for nanoparticles[4] and this method has been extended by Campbell and Fauchet to nanowires.[5] This model has been applied by many experimental groups to explain the observed asymmetry of the phonon bands in their nanowire Raman spectra. Silicon is the perfect testing ground for the physics of phonon confinement. Yet in this nanowire system alone, the results connecting nanowire diameter and asymmetric broadening of the 520 cm^{-1} LO-TO phonon band are not consistent.[6–18] Only recently has a systematic study of the line asymmetry vs nanowire diameter been reported.[19] We believe that the quantitative differences between this recent work in Si nanowires[19] and other Si nanowire results[6–18] indicate that a second mechanism, beyond phonon confinement, is responsible for the discrepancies in the literature. From two previously published papers, there indeed is a clear case for a laser-flux-induced second mechanism. One work attributed the increase in A with flux to Fano interference scattering from photogenerated free carriers,[18] and the other to thermal effects and inhomogeneous heating.[11] In previous work on the laser flux-induced Raman line asymmetry in Si nanowires,[18] we noted that a Breit-Wigner-Fano line shape provided a reasonably good fit to the data. This success led us to propose that we were observing a photoexcitation rather than a thermal phenomenon. Subsequent experiments were then designed to further test the photoexcitation hypothesis. The results are presented here. In these experiments, the same intensity beam was presented to Si nanowires with differing thermal coupling to the underlying substrate. The results of these studies, to be presented below, showed that the asymmetric line broadening with increasing laser flux is a thermal phenomenon. We show below that the additional asymmetry is not due to homogenous heating, but to inhomogeneous heating.

In this paper, we present results of a systematic study of the observed changes in line asymmetry A with laser flux Φ in Si nanowires of known diameter. We also have investigated how these changes in $A(\Phi)$ relate to the thermal connection of the nanowire to the underlying substrate. Here we present convincing theoretical arguments that show that significant temperature gradients in the Raman scattering volume induced by the excitation laser can contribute to the line asymmetry. The gradients are the result of a thermal bottleneck that prevents energy deposited by the laser in the Raman volume from diffusing away. Recent thermal conductivity studies by Li *et al.*[20] show that the thermal conductivity of Si nanowires is significantly suppressed relative to the bulk. This suppression was identified[20] with the importance of surface scattering of the long wavelength acoustic phonons.

An inhomogeneous heating effect was proposed earlier by Piscanec *et al.* to explain their observed growth in A with increasing laser flux Φ in Si nanowires.[11] However, they did

not present a line shape analysis to support their proposal, nor did they investigate the role of the thermal connection of the nanowires to the substrate. By using the Richter line shape function extended to include the effects of a temperature distribution, we can obtain a semiquantitative understanding of inhomogeneous laser heating phenomena and Raman scattering in nanowires.

EXPERIMENTAL DETAILS

Crystalline Si nanowires were synthesized by a pulsed laser vaporization of Si:Fe target in flowing $Ar:H_2$.[13,21] Details of our synthesis procedure have already been published.[18] Briefly, a target of Si:10% Fe in a quartz tube maintained at 1200 °C in flowing $Ar/10\%H_2$ was ablated with a pulsed Nd:YAG laser (Spectron Laser systems) that was focused to a ~2 mm spot on the target (simultaneously present: 1064 nm at 950 mJ/pulse, and 532 nm at 320 mJ/pulse). To make smaller diameter nanowires, the nanowires were oxidized *in situ* at 500–700 °C in a pure (and dry) oxygen flow. Oxygen then diffuses through the cylindrical boundary of the nanowire and "shrinks" the diameter of the crystalline core. Details of this technique will appear elsewhere.[22]

To make a sample for Raman scattering studies, a suspension of the nanowires in isopropanol was prepared by agitation in an ultrasonic bath for 30 min (VWR, model P250HT) followed by an ultrasonic horn for 5 min (Misinix Inc. model No. XL 2010) operated at 100 W. This suspension was allowed to settle; large Si particles and large diameter Si nanowires formed a sediment. The supernatant was then decanted and separated into samples, or "cuts," with differing mean diameter using a centrifugal separation method described in detail elsewhere.[22] In this way, Si nanowire samples with very different and reasonably narrow diameter distributions were prepared. One of these samples studied here has a population of primarily large diameter wires ($\bar{d}$=23 nm) so that very weak phonon confinement effects are expected in this sample on the basis of the Richter model. At high flux, the one-phonon Raman band from this sample departs noticeably from a symmetric (Lorentzian) line shape.

Samples were prepared for micro-Raman experiments in air (under ambient conditions) by placing 2–3 drops of solution containing the suspended Si nanowires onto a $5\times5\times0.1$ mm^3 piece of indium foil. The isopropanol was then allowed to evaporate at room temperature. Indium foil was chosen because it is a good thermal conductor, does not absorb much of the laser radiation, and does not exhibit a Raman spectrum. Raman scattering spectra were collected from regions with high and low wire density on the indium substrate, as determined by optical microscope observations with the incident laser light. Low wire density, or low coverage on the substrate, promoted good thermal anchoring of the wires to the substrate, whereas high coverage means that wires are suspended by other wires above the indium foil and, as such, many are in poor thermal contact with the substrate. These self-suspended wires are much more easily heated in the intense radiation present in the micro-Raman apparatus.

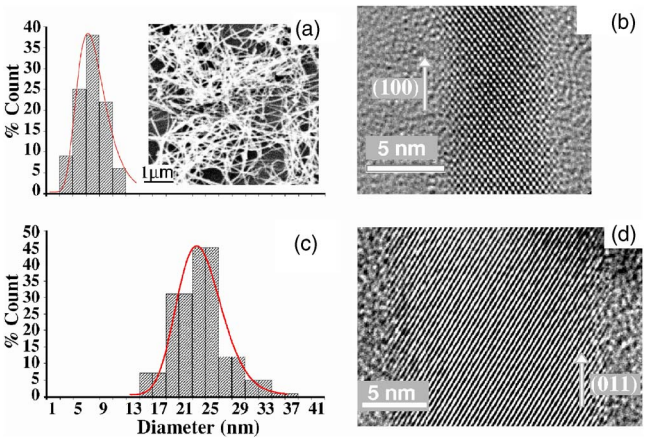

FIG. 1. (Color online) (a,c) The diameter distribution of the Si crystalline core for $\bar{d}$=6 nm (a) and $\bar{d}$=23 nm (c) nanowires. The solid curve in (a,c) is a log-normal fit to the distribution. The inset in (a) is the SEM image of the wires on In foil substrate. (b,d) The HRTEM image of a 7 nm wire and 16 nm wire, respectively.

The Raman spectra were collected in air using an argon ion laser in the backscattering geometry using a JY-ISA T64000 spectrometer equipped with an Olympus BX40 confocal microscope and 100X objective (~1 μ diameter focal spot size). The laser power at the sample was measured using a miniature hand-held radiometer.

The diameter distribution of the crystalline Si core in our wire samples was measured by high-resolution transmission electron microscopy (HRTEM) using a JEOL (JEM 2010F) microscope at 200 kV. The wires were observed to be covered with an amorphous SiO_x coating. The diameter distribution we report here refers to that of the central crystalline Si core. Scanning electron microscopy (SEM) images of the nanowires were taken with an Hitachi S3500N microscope.

RESULTS AND DISCUSSION

In Figs. 1(a) and 1(c) we show the diameter distribution of the crystalline Si core of two sets of silicon nanowires used in this micro-Raman study. The solid curve in the figure is a fit to the measured diameter distribution by a log-normal function $F(d)=\frac{1}{\sigma}\exp-[(\log d-\log\bar{d})^2/2\sigma^2]$ (Ref. 23) with ($\bar{d}$=6 nm, σ=1.38) and ($\bar{d}$=23 nm, σ=2.85). From HRTEM images [see Figs. 1(b) and 1(d)], we observed a highly crystalline core in the center of our nanowires, surrounded by a several-nm-thick amorphous SiO_x shell. No dominant growth direction was observed [i.e., growth occurs along (111), (100) and (011) directions].

We collected Raman spectra from regions on the indium foil where Si wires were found in either a "high" or "low" coverage state (i.e., coverage refers to the density of nanowires per unit area on the indium foil substrate). By high coverage, we mean a distribution similar to (or denser than) that shown in the (SEM) image in Fig. 1(a) (inset). At high coverage, many of the nanowires are essentially suspended by each other. As a result, they are not in good thermal contact with the substrate and are more easily heated by the

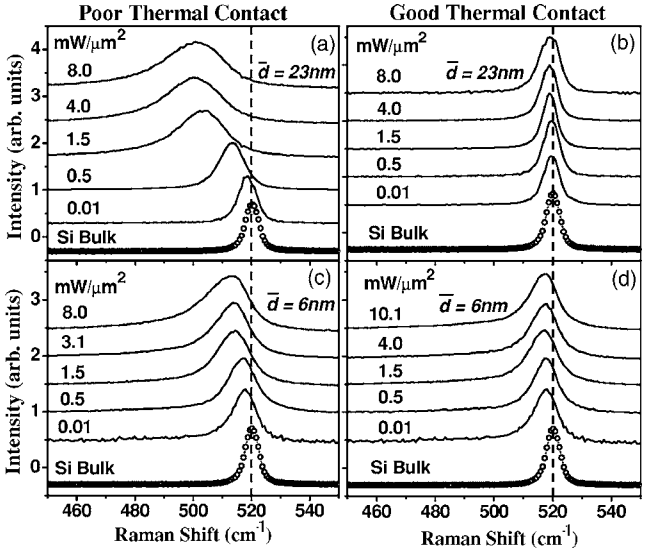

FIG. 2. Flux dependent-Raman spectra of Si nanowires on indium substrate collected under poor thermal anchorage (a,c) and good thermal anchorage (b,d) for 23 nm wires (a,b) and 6 nm wire (c,d). Spectra were collected using 514.5 nm radiation.

micro-Raman laser beam. By low coverage, we mean a submonolayer coverage, where most wires are in direct contact with the substrate.

In Fig. 2, we display the evolution of the 520 cm^{-1} one-phonon Raman band with increasing laser flux Φ for $\bar{d}=23$ nm wires [Figs. 2(a) and 2(b)] and for $\bar{d}=6$ nm wires [Figs. 2(c) and 2(d)]. The spectra are stacked from bottom to top with increasing laser flux; the spectrum of bulk Si (taken at low laser flux) is on the bottom for comparison. For a visual guide, a vertical reference line is drawn at 520 cm^{-1}, so that the shift in the Raman peak with laser flux is more apparent. Spectra from regions of low and high coverage are displayed. In Figs. 2(b) and 2(d), the evolution of the 520 cm^{-1} Raman band with increasing Φ from wires with submonolayer coverage (good thermal contact) is presented: $\bar{d}=23$ nm [Fig. 2(b)] and $\bar{d}=6$ nm [Fig. 2(d)]. The shifting and broadening of the spectra with increasing laser flux is evident in the figure. However, a careful line shape asymmetry analysis is required to identify the more subtle changes in line shape that are occurring with increasing laser flux. This analysis is described below after we discuss the Richter model. Figures 2(a,c) present results for $\bar{d}=23$ nm (a) and $\bar{d}=6$ nm (b) that makes poor thermal contact with the substrate. In this case, the spectral changes with increasing Φ are much more evident.

We now briefly introduce the phonon confinement model proposed by Richter, Wang, and Ley[4] to interpret the asymmetric Raman line shape observed in small semiconducting particles. The work was extended to wires and films by Campbell and Fauchet.[5] For the case of Si nanowires, the Raman scattering intensity $I(\omega)$ at photon frequency ω measured relative to the laser frequency is given by[4,5]

$$I(\omega) = I_o \int_o^1 2\pi q_\perp \mathrm{d}q_\perp \frac{|C(q_\perp)|^2}{[\omega - \omega_o(q_\perp, T)]^2 + (\Gamma(T)/2)^2}. \quad (1)$$

$$|C(q_\perp)|^2 = C_o \exp\{-(1/2)[q_\perp d/\alpha a_o]^2\}, \quad (2)$$

where d and a_0 are, respectively, the wire diameter and the lattice constant for Si. The line shape function $I(\omega)$ in Eq. (1) involves an integral over the confined phonons of the infinite solid (bulk Si) with *normalized* wave vector $q_\perp$ perpendicular to the wire axis, i.e., $q_\perp$ runs over the range $0<q_\perp<1$ in the Brillouin zone. Equation (1) is then seen to be a sum of Lorentzian contributions from each bulk phonon with wave vector $\boldsymbol{q}=(q_\perp, q_{||}=0)$, where $q_{||}$ is the component of the phonon wave vector parallel to the nanowire axis. Therefore, using bulk states for the description of the $q=0$ confined phonon in the nanowires, the Richter model requires that a superposition of *bulk* phonons over a range of $q_\perp$ be used. This is similar in form to the result which can be derived for wave packets, i.e., $\Delta q(\Delta x=d)\sim 1$, where Δq is the range of wave vector required to describe the localization of a particle to a region of width d. Note that both the phonon frequency $\omega_o(q_\perp)$ and lifetime $1/\Gamma$ in Eq. (1) are given an explicit temperature (T) dependence. This will be shown to be important later, when we consider inhomogeneous laser heating phenomena.

The Gaussian confinement function $|C(q_\perp)|^2$ [shown in Eq. (2)] is the result of the Richter model assumption that a Gaussian envelope in real space attenuates the phonon amplitude with increasing distance r from the nanowire axis. The quantity α [Eq. (2)] did not appear as a physical variable in the paper by Richter, Wang, and Ley and there does not appear to be a reason for their choice of $\alpha=1.4$. Therefore, in subsequent work[19] we introduced α as a parameter to be determined by experiment (it sets the scale for the confinement relative to the wire diameter d).

To carry out the integration in Eq. (1), we use an isotropic form for $\omega_o(q_\perp)$ determined from neutron scattering experiments on bulk Si; it is given by[24]

$$\omega(q_\perp) = \left[A + B\cos\left(\frac{\pi q_\perp}{2}\right)\right]^{\frac{1}{2}}, \quad (3)$$

where $A=1.714\times10^5$ cm^{-2} and $B=1.0\times10^5$ cm^{-2}. In cases where the Raman scattering intensity is simultaneously collected from many wires, the measured diameter distribution of the nanowires can be used to further refine the analysis of the Raman line shape.[19] Using the measured nanowire diameter distributions [obtained by statistical analysis of TEM images], we found earlier[19] that the universal value $\alpha=6.3\pm0.2$ in Eq. (1) was needed to fit the Richter model line shape to data collected for four wire ensembles with mean diameter that spanned the range 4.5 nm$\leqslant\bar{d}\leqslant$23 nm. Ignoring the diameter distribution (i.e., using only the mean diameter $\bar{d}$ in the Richter analysis), leads to a somewhat larger value for α.[19] For our Si nanowires, the diameter distribution is reasonably narrow, and as such it is relatively unimportant in the analysis here. We have discussed the effect of the diameter distribution on the line shape of Si 520 cm^{-1} line in a previous publication.[19] In Fig. 3, we show the Raman line shape predicted for the $q_{||}=0$ optical phonons in Si nanowires [Eq. (1)] for $\alpha=6.3$, omitting the diameter distribution. A value for the inverse phonon lifetime of

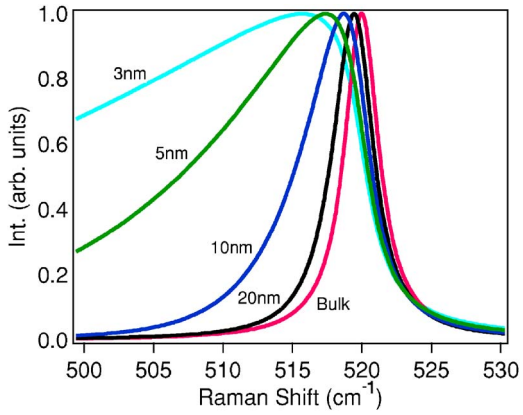

FIG. 3. (Color online) Calculated Raman line shapes for different diameters of Si nanowires as predicted by the phonon confinement model of Richter [Eq. (1)] (see Ref. 4). The line shapes develop asymmetrically and downshift with decreasing diameter.

$\Gamma=4.7$ cm^{-1} (full width at half maximum) was used in Eq. (1) which includes the effects of our instrumental broadening.[25] It can be seen that with decreasing wire diameter d (i.e., *increasing* confinement), the one-phonon $\sim$520 cm^{-1} Raman band in Si asymmetrically broadens to lower frequency; the band maximum also downshifts in frequency. It is also clear that a $d=20$ nm nanowire exhibits a weak signature of phonon confinement, i.e., the line shape is almost Lorentzian.

In order to study the effects of the incident laser flux on the asymmetry in the $\sim$520 cm^{-1} band *without* using Richter's line shape function [Eq. (1)], we have constructed a phenomenological measure of the Raman band asymmetry A that is commonly used in liquid chromatography.[26] Later we will fit the spectra in Fig. 2 using the Richter line shape function suitably modified to include inhomogeneous heating. We define the band asymmetry A as the ratio of the widths ($\Delta\omega$) at 10% of maximum intensity measured relative to the band maximum (cf., Fig. 4). Specifically, A is given by

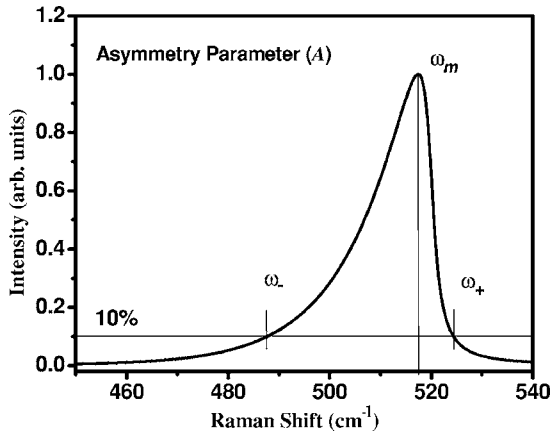

FIG. 4. Definition of the asymmetry parameter A [Eq. (4)] (see Ref. 26) used in our analysis.

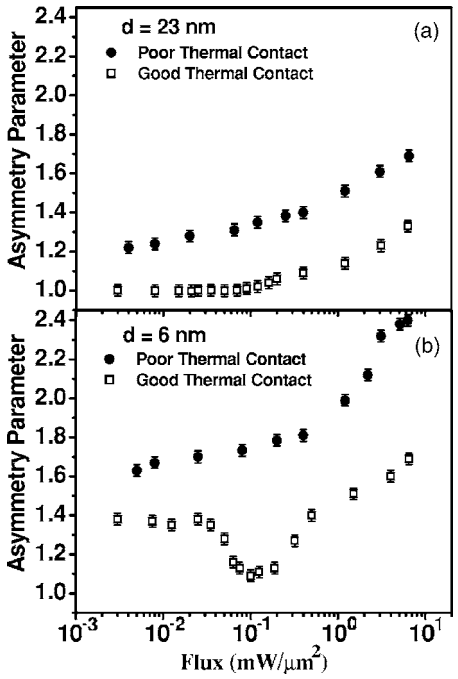

FIG. 5. Flux (Φ) dependence of the asymmetry parameter for Si nanowires under poor thermal contact (solid circles) and good thermal contact (open squares) for (a) 23 nm, (b) 6 nm Si nanowires. Raman spectra were collected using 514.5 nm radiation.

$$A = \frac{\Delta\omega_L}{\Delta\omega_R} = \frac{\omega_m - \omega_-}{\omega_+ - \omega_m}, \tag{4}$$

where the subscripts L, R refer to the left and right widths at 10% intensity, respectively. The frequencies ω_- and ω_+ locate the positions at 10% intensity on the low and high frequency sides of the band maximum ω_m. We use this definition for A because it is sensitive to the subtle changes in the Raman band asymmetry and, furthermore, does not require a fit of the line shape to a specific function. It should be noted that $A=1$ is obtained for a symmetric line shape, e.g., a Lorentzian.

Values for the asymmetry parameter A for spectra that appear in Figs. 2(a)–2(d) (and others) were obtained according to the criterion given in Eq. (4), and the behavior of A vs Φ, where Φ is the laser power per unit area in the focal plane of the micro-Raman instrument, was obtained. These results are shown in Fig. 5. The laser power was measured at the position of the sample using a small (hand-held) radiometer inserted between the objective and the microscope stage; the 100x objective that we used illuminates an area of $\sim 1\ \mu^2$. In Fig. 5(a), we display our $A(\Phi)$ data for the $\bar{d}=23$ nm wires; the open squares and the solid circles refer to low and high coverage of these nanowires on the indium foil, respectively. At low Φ, the data for high wire coverage on the substrate (poor thermal contact) exhibits a monatonic increase in A vs Φ. Conversely, data from low coverage regions at low Φ exhibits a Φ-independent A (for $\Phi<70\ \mu\mathrm{W}/\mu\mathrm{m}^2$). The value $A\sim 1$ obtained at low Φ for $\bar{d}=23$ nm Si nanowires is consistent with the Richter model ($\alpha=6.3$) and indicates that

these wires are too large to observe a significant phonon confinement distortion of the 520 cm^{-1} band. Furthermore, for $\Phi > 70\ \mu W/\mu m^2$, A in these large diameter wires begins to increase with increasing Φ. *This increase in A with* Φ *cannot be related to phonon confinement, and must be attributed to some other mechanism* (as we discuss below).

In Fig. 5(b), we display A vs Φ for low and high Si nanowire coverage on the indium foil substrate, but for the smaller diameter ($\bar{d}=6$ nm) wires. As in Fig. 5(a), the open squares and the solid circles refer, respectively, to low and high coverage on the indium foil. As can be seen in Fig. 5 by comparing the behavior of $A(\Phi)$ for large and small diameter wires at a specific coverage, or by comparing $A(\Phi)$ for a given mean wire diameter and low coverage vs high coverage, interesting and contrasting behavior is observed.

Just after the introduction of high power Ar ion lasers, strong deviations from a symmetric Lorentzian line shape were reported for the one-phonon Raman band in bulk Si.[27] Using a tightly focused laser beam, an asymmetric broadening to lower frequency was reported for the 520 cm^{-1} band and attributed to inhomogeneous heating within the Raman volume. However, no analysis of the asymmetric line shape was provided in that work. Similarly, in the case of Si nanowires, a growing asymmetry of the 520 cm^{-1} Raman band with increasing laser flux has also been reported.[11,18] Piscanec *et al.*[11] identified the asymmetry with inhomogeneous laser heating, but did not provide a quantitative analysis of their asymmetric line shape, nor were they able to separate out the individual contributions that might come from phonon confinement and inhomogeneous heating effects. Below, we show that the proposal of Piscanec *et al.* is probably correct, and that all the interesting behavior we observe for $A(\Phi)$ in Si nanowires (shown in Fig. 5) can be understood on the basis of the Richter model if a spatial temperature dependence $T(z)$ along the wire axis is introduced.

To extend the Richter model calculation to handle a $T(z)$, we need to introduce the temperature dependence of the relevant Si phonon parameters obtained from careful studies of the bulk. With increasing T, the *inverse* optical phonon lifetime Γ for $q=0$ increases due to anharmonic interactions.[28]

$$\Gamma(T) = C_1\left(1 + \frac{2}{\exp(\hbar\omega_o/2k_BT) - 1}\right) + C_2\left(1 + \frac{3}{\exp(\hbar\omega_o/3k_BT) - 1} + \frac{3}{[\exp(\hbar\omega_o/3k_BT) - 1]^2}\right), \tag{5}$$

where $C_1 = 1.295\ cm^{-1}$ and $C_2 = 0.105\ cm^{-1}$. The Si phonon frequencies, on the other hand, decrease due to thermal expansion.[28] For the optic phonons at $q=0$, the T dependence is given by[28]

$$\Delta\omega_o = C_3\left(1 + \frac{2}{\exp(\hbar\omega_o/2k_BT) - 1}\right) + C_4\left(1 + \frac{3}{\exp(\hbar\omega_o/3k_BT) - 1} + \frac{3}{[\exp(\hbar\omega_o/3k_BT) - 1]^2}\right), \tag{6}$$

where $C_3 = -2.96\ cm^{-1}$ and $C_4 = -0.174\ cm^{-1}$. As an approximation, we take the temperature dependence of Eqs. (5) and (6) to be typical of the behavior of other phonons throughout the Brillouin zone and introduce it into the Richter model [Eq. (1)]. If the heating is uniform, the effect of temperature in Eqs. (5) and (6) can be shown to homogeneously broaden the Raman line. However, if temperature gradients exist along the wire, we must carry out an additional integration along the wire axis (z). We take the intensity distribution of the laser beam along a wire in the focal spot to be a Gaussian described by[29]

$$I(z) = I_o \exp\left(-\frac{z}{a}\right)^2, \tag{7}$$

where a is related to the focal spot size in the Raman experiment ($a \sim 1\ \mu$ and $a \ll$ wire length). We also assume that a Gaussian temperature distribution $T(z)$ is induced along the wires via the competition between laser heating and thermal cooling due to the coupling of the nanowire to the substrate and the ambient

$$T(z) = \Delta T \exp\left(-\frac{z}{b}\right)^2 + T_a, \tag{8}$$

where ΔT describes the maximum temperature rise above the ambient temperature background (i.e., $T_a \sim 300$ K), and the parameter b describes the width of the induced temperature profile along the nanowire axis (z). Including both the laser intensity distribution $I(z)$ and the induced temperature response $T(z)$ in the Richter model [Eq. (1)] leads to the following line shape function:

$$I(\omega) = \int_{-c}^{+c} dz I_o e^{-(z/a)^2} \int_o^1 2\pi q_\perp dq_\perp \times \frac{|C(q_\perp)|^2}{[\omega - \omega_o(q_\perp, T(z))]^2 + [\Gamma(T(z))/2]^2}. \tag{9}$$

The integral in z is calculated over the average length of a nanowire ($l=2c$) from which Raman scattered radiation can be imaged through the slit of the spectrometer ($\sim 1\ \mu$), the integral over $q_\perp$ is the same as in Eq. (1). As we show below, Eq. (9) and the T-dependent phonon properties of bulk Si can explain qualitatively the $A(\Phi)$ behavior shown in Fig. 5. Plotting calculated results from Eq. (9) shows that the increase in the band asymmetry A due to inhomogeneous heating is identified with the contribution from the spatial dependence of the phonon frequency in the integral. The spatial dependence of Γ actually offsets some of this line shape asymmetry.

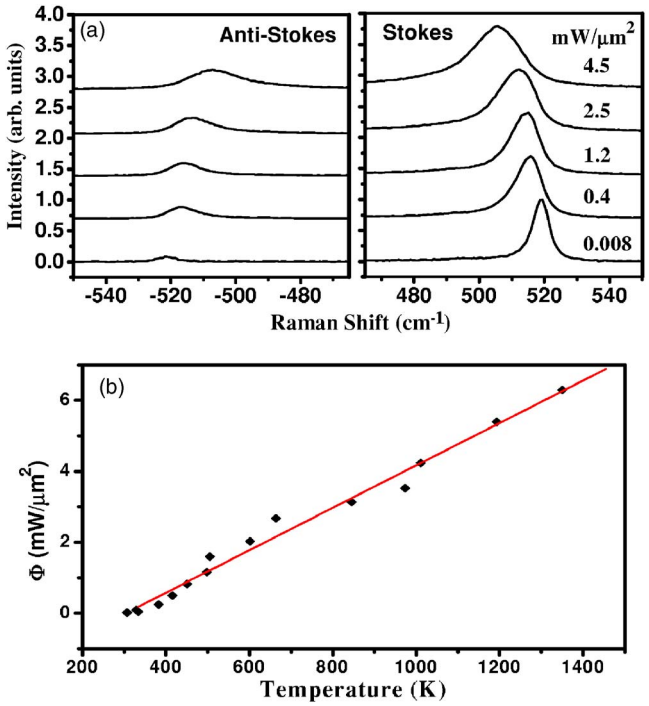

FIG. 6. (Color online) (a) Stokes-antiStokes spectra of 23 nm Si nanowires collected at high wire coverage and, (b) flux vs T_{eff} in Raman volume calculated using Eq. (10). Spectra were collected using 514.5 nm excitation.

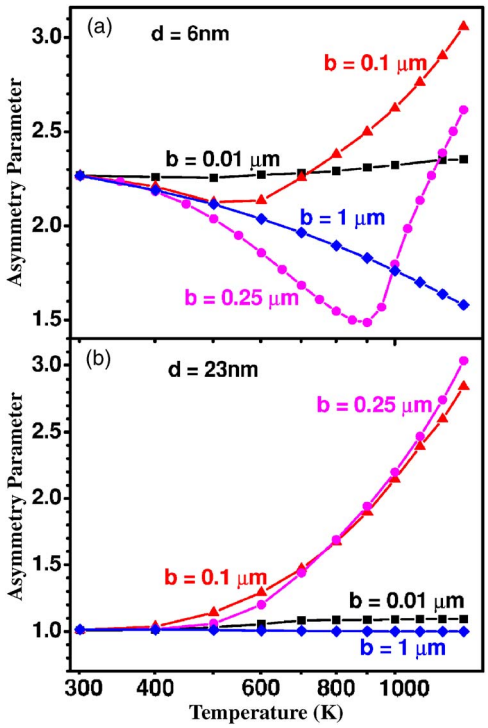

FIG. 7. (Color online) Calculated asymmetry parameter of the Raman line shape [Eq. (9)] vs temperature for: (a) 6 nm and (b) 23 nm Si nanowires for different temperature profiles: b=0.01 μ (solid squares), 0.1 μ (solid triangle), 0.25 μ (solid circles) and 1.0 μ (solid diamonds).

Before examining the particular $A(\Phi)$ behavior that stems from inhomogeneous heating, we need experimental estimates for the maximum temperature rise due to laser heating (ΔT). We have measured the Stokes-AntiStoke scattering ratio (I_S/I_{AS}) that is related to the temperature T_{eff} in the Raman scattering volume by

$$\frac{I_S}{I_{AS}} = \beta e^{-\frac{\hbar\omega_o}{k_B T_{eff}}}. \tag{10}$$

In Fig. 6, for $\bar{d}$=23 nm wires, we plot Φ vs T_{eff} from the experimentally determined I_S/I_{AS}, where T_{eff} represents an effective temperature in the Raman volume of the nanowires as determined by application of Eq. (10). As can be seen, an approximately linear relationship between Φ and T_{eff} is obtained. Furthermore, it is interesting that nanowire temperatures exceeding 1000 K can be obtained, as reported previously by Gupta *et al.*[18]

We now present the results of our calculations for the effects of inhomogeneous heating on the band asymmetry parameter A. We have used Eqs (5)–(9) with α=6.3 to calculate the effect of the induced temperature distribution $T(z)$ within the confines of our simple extension of Richter's model. The results of our analysis are plotted in Fig. 7 as A vs log T^*($T^*=\Delta T+T_a, T_a$=300 K, ΔT is the maximum temperature rise in the wire). It is reasonable to believe that $\Delta T+T_a \sim T_{eff}$, and we should recall that T_{eff} has been shown experimentally (cf., Fig. 6) to be linear in the incident laser flux Φ. So, for comparison with the A vs log Φ data in Fig. 5, we have plotted the calculated results of A vs log T^* in Fig. 7.

Shown in Fig. 7(a) are our calculated results for the smaller diameter d=6 nm wires, and for four different values of b that describe the Gaussian width of the temperature distribution induced by the focused laser beam. At the lowest values of ΔT (i.e., consistent with low Φ), we recover the value of the asymmetry parameter $A \sim 2$ which is due to phonon confinement without heating. With increasing flux, four distinct behaviors for $A(\Phi)$ can be observed that depend on the choice of b. In the limit of a very sharp $T(z)$, indicated by the squares, A is found to be almost independent of ΔT. A very sharp $T(z)$ is an unphysical situation, and is plotted here only for completeness. In this case, only a small fraction of the nanowire is significantly heated (and imaged onto the spectrometer slit) and the remainder of the nanowire that can be imaged into the slit is not found in much of a temperature gradient. On the other hand, for larger values of b, either a monatonic or a nonmonatonic behavior of A with increasing ΔT is observed for these 6 nm wires, in agreement with the experimental data $A(\Phi)$ shown in Fig. 5. It should be noted that a relatively sharp $T(z)$ should be identified with the experimental condition of high nanowire coverage on the indium foil, and the concomitant poor thermal anchoring of the wires to the substrate. A relatively broad $T(z)$ should be identified with low coverage and better thermal contact to the substrate. In Fig. 7(a), one can observe the calculated [Eq. (9)] nonmonatonic behavior for b=0.25 μ similar to that observed experimentally for 6 nm wires at low wire coverage

on the indium foil. The inhomogeneous laser heating first causes a decrease in A, followed by an increase. For 6 nm diameter wires exposed to the broadest temperature distribution (i.e., $b=1.0\ \mu$), we calculated that A exhibits a monatonic decrease with increasing ΔT induced by the laser. In this case, a broad $T(z)$ generates behavior similar to what we would expect for homogeneous heating of the nanowire. That is, the temperature-induced broadening of the individual Lorentzian components (via increasing Γ) in the integrals Eqs. (1) and (9) reduces the line asymmetry and overshadows the opposite contribution from the temperature gradients within the Raman volume [via the $\omega_o(T)$ factor].

In Fig. 7(b), we show the results of our calculations for a large diameter $d=23$ nm Si nanowire. In this case, most of the Raman band asymmetry should be ascribed to inhomogeneous heating (and almost none to phonon confinement). Again, we use $a=0.5\ \mu$ for the laser spot parameter and $\alpha=6.3$. As can be seen, the $d=23$ nm wire is large enough for $A\sim 1$ at low Φ. For $b=0.25\ \mu$, (circles) and $b=0.1\ \mu$, (triangles), A is seen to increase dramatically with increasing ΔT. It should be noted that for the $d=23$ nm wire, we do not observe the experimental "dip" in $A(\Phi)$ seen for the 6 nm wire. From our calculations we now understand that this dip is due to the interplay of phonon confinement and inhomogeneous heating.

To put the above analysis in perspective, we next used the modified Richter line shape function Eq. (9) to directly fit the experimental spectra for the 520 cm^{-1} band of $d=6$ nm nanowires at $\Phi=0.01$,0.5,and 2.5 $mW/\mu m^2$ and for $d=23$ nm nanowires for $\Phi=0.01$,2.0,and 4.0 $mW/\mu m^2$. We have fixed $a=0.5\ \mu$, $b=0.25\ \mu$, $\alpha=6.3$. ΔT is the only adjustable parameter in our spectral line shape analysis. The data and least squares fit [Eq. (9)] for $d=6$ nm and $d=23$ nm Si wires appear in Fig. 8 (middle and bottom panels), respectively. The open circles are the Raman data and the least squares fit of the modified Richter model [Eq.(9)] is represented by the solid curve. For the 6 nm wires (middle panel, Fig. 8), we obtained $\Delta T=45$, 190, and 380 K for $\Phi=0.01$, 0.5, and 2.5 $mW/\mu m^2$, respectively. Similarly, for the 23 nm wires (bottom panel, Fig. 8), we obtained $\Delta T=30$, 350, and 750 K for $\Phi=0.01$, 2.0, and 4.0 $mW/\mu m^2$, respectively. As can be seen from the least squares fit to the experimental spectra, the line shape function [Eq. (9)] provides a reasonably good fit to the Raman data.

To further substantiate the values of ΔT obtained from the least squares fit (Fig. 8), we now return to a more exact analysis of the Stokes-antiSokes intensity ratio. These scattering intensities, as derived for an inhomogeneously illuminated and heated Raman volume, are given by

$$I_S \cong \beta' \int_{-l/2}^{l/2} I_o e^{-\left(\frac{z}{a}\right)^2} [n(\omega_o, T(z)) + 1] dz,$$

$$I_{AS} \cong \beta'' \int_{-l/2}^{l/2} I_o e^{-\left(\frac{z}{a}\right)^2} n(\omega_o, T(z)) dz, \qquad (11)$$

where $n(\omega_o, T(z))$ is the equilibrium occupation number of the $q=0$ optical phonons of frequency ω_o. β' and β'' depend on the scattering cross section, optical absorption constant,

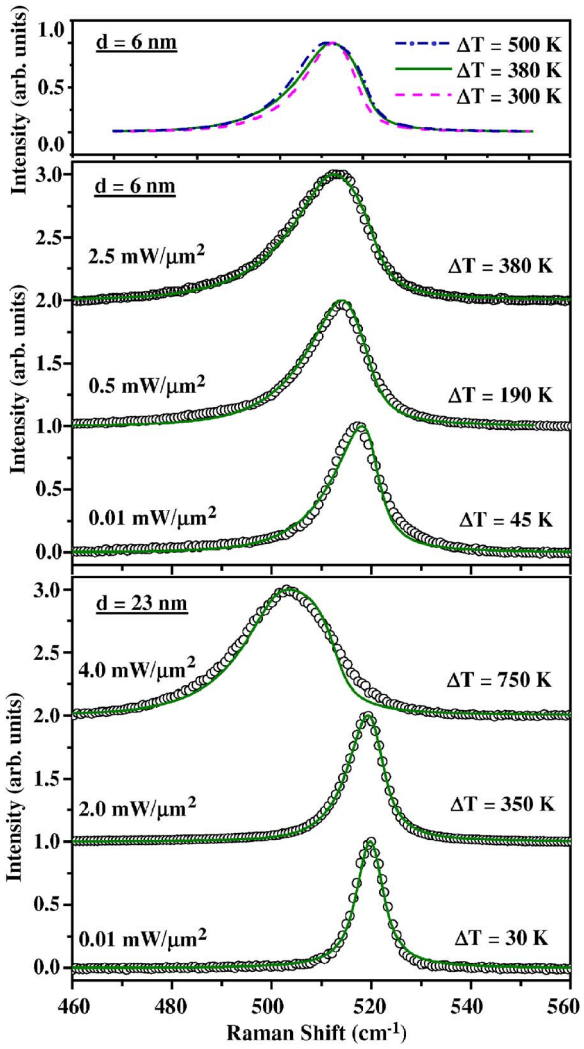

FIG. 8. (Color online) Raman spectra (open circles) for the $\bar{d}=6$ nm (middle panel) and $\bar{d}=23$ nm (bottom panel) Si nanowires collected at 514.5 nm excitation. The solid lines are calculated according to Eq. (9) for parameter values given in the text. ΔT is the maximum increase in the sample temperature found from the line shape analysis. Values for the experimental laser flux are indicated. The top panel shows the sensitivity of the calculated line shape function to the values of ΔT [Eq. (9)]; all other parameters are fixed ($\alpha=6.3$, $a=0.5\ \mu$, $b=0.25\ \mu$).

and the Raleigh factor at the Stokes and antiStokes frequencies, respectively. The rest of the variables are as defined previously. To fit the data we require that $(\beta'/\beta'')\sim 0.8$ at 300 K (ambient sample temperature). Using Eq. (11), $a=0.5\ \mu$, $b=0.25\ \mu$ and the value of ΔT obtained from the fits displayed in Fig. 8, we have calculated (I_S/I_{AS}) for the 23 nm Si nanowire for $\Phi=0.01$, 2.0, and 4.0 $mW/\mu m^2$.The results are shown in Table I, where they are compared to experiment. As can be seen, we find a very good agreement between measured and calculated I_S/I_{AS} for low heating. However, with increasing induced temperature, a systematic, but small disagreement between the calculated and experimental Stokes-antiStokes ratio develops. This can be identified with our simplifying assumption of a fixed $b=0.25\ \mu$ in

TABLE I. Results calculated from Stokes and antiStokes scattering from the 520 cm^{-1} LO-TO band of $\bar{d}$=23 nm diameter wires vs laser flux. T^* is the maximum sample temperature in the center of the focal spot determined from a line shape analysis of the Stokes band using Eq. (9). T_{eff} is the effective average temperature in the Raman volume obtained from the Stokes-antiStokes intensity ratio.

$\bar{d}$(nm)	Φ (mW/μm^2)	$T^*(K)$[a]	$T_{eff}(K)$[b]	$T^*-T_{eff}(K)$	(I_S/I_{AS}) Calc.[c]	Expt.
23	0.01	330	310	20	10.7	11.1
	2.0	650	600	50	4.6	5.0
	4.0	1050	950	100	3.1	4.0

[a]Calculated from fitting modified Richter function Eq. (9) to experimental line shape.
[b]Calculated using Eq. (10) and experimental I_S/I_{AS}.
[c]Calculated using Eq. (11) and ΔT obtained form the line shape fitting shown in Fig. 8.

our calculation of I_S/I_{AS}. In actuality, b is expected to be temperature dependent and should increase with increasing temperature. Also shown in Table I is a comparison of T^* and T_{eff}, where T^* is obtained from the line shape fitting using Eq. (9) and the sample temperature T_{eff} obtained from the analysis of the Stokes-antiStokes ratio [Eq. (11)]. We find that the difference in these temperatures ranges from ~20 to 100 K, which is comparable to the estimated error in T^* obtained from the line shape analysis. We give some visual indication of the sensitivity of the line shape analysis to T^* by plotting the calculated line shape for $\bar{d}$=6 nm with T^* =600, 700, and 800 K. These results are shown in the top panel of Fig. 8.

Finally, we should mention that our diameter distributions are narrow enough that the effect on the line shape is overshadowed by inhomogeneous heating. We can make this conclusion based on line shape calculations [Richter model, Eq. (9)] with and without the inclusion of the diameter distribution. These calculations showed that the change in asymmetry induced by the diameter distribution was small compared to that contributed by the inhomogeneous heating.

SUMMARY AND CONCLUSIONS

We have shown experimentally that the Φ dependence of the 520 cm^{-1} Raman band asymmetry A in Si nanowires depends *both* on the nanowire diameter and on inhomogeneous heating within the Raman scattering volume. A variety of monatonic and nonmonatonic behaviors for $A(\Phi)$ can be observed, depending on the wire diameter and thermal sinking of the wires to the substrate. Similar $A(\Phi)$ behaviors to that observed experimentally can be *calculated* using an extension of the Richter model to include the effects of a laser-induced temperature distribution in the nanowires. Furthermore, we have used the modified Richter model to fit the experimental line shape using only one additional parameter (ΔT, or the maximum temperature increase in the wire induced by laser heating). Thus, our results support the original proposal by Piscanec *et al.*[11] that an asymmetric line shape of the 520 cm^{-1} band can develop due to an inhomogeneous laser heating in the nanowires. We conclude that two contributions to the Raman line asymmetry (i.e., phonon confinement and inhomogeneous heating) can be separated by studying the flux dependence of the line asymmetry. If Raman scattering is to be used to study pure phonon confinement effects in nanowires, high thermal conductivity substrates and low nanowire coverage over the substrates are preferred.

ACKNOWLEDGMENTS

The authors gratefully acknowledge stimulating conversations with Gerald Mahan (Pennsylvania State University) and José Menéndez (Arizona State University). This work was supported, in part, by funding from the NSF (NIRT No. DMR-0304178).

*Corresponding author; electronic address: pce3@psu.edu

[1] A. D. Yoffe, Adv. Phys. **42**, 173 (1993).
[2] A. D. Yoffe, Adv. Phys., **50**, 1 (2001).
[3] D. D. D. Ma, C. S. Lee, F. C. K. Au, S. Y. Tong, and S. T. Lee, Science **299**, 1874 (2003).
[4] H. Richter, Z. P. Wang, and Y. Ley, Solid State Commun. **39**, 625 (1981).
[5] I. H. Campbell and P. M. Fauchet, Solid State Commun. **58**, 739 (1986).
[6] S. Bhattacharyya and S. Samui, Appl. Phys. Lett. **84**, 1564 (2004).
[7] L. Jianxun, N. Jujie, Y. Deren, Y. Mi, and S. Jian, Physica E (Amsterdam) **23**, 221 (2004).
[8] S. Hofmann, C. Ducati, R. J. Neill, S. Piscanec, and A. C. Ferrari, J. Appl. Phys. **94**, 6005 (2003).
[9] B. Li, D. Yu, and S. L. Zhang, Phys. Rev. B **59**, 1645 (1999).
[10] F.-M. Liu, W. Tian-Min, Z. Li-De, Chin. Phys. **13**, 2169 (2004).
[11] S. Piscanec, M. Cantoro, A. C. Ferrari, J. A. Zapien, Y. Lifshift, S. T. Lee, S. Hofmann, and J. Robertson, Phys. Rev. B **68**, 241312 (2003).

[12] W. F. Zhang, Y. L. He, M. S. Zhang, Z. Yin, and Q. Chen, J. Phys. D **33**, 912 (2000).
[13] Y. F. Zang, Y. H. Tang, N. Wang, D. P. Yu, C. S. Lee, I. Bello, and S. T. Lee, Appl. Phys. Lett. **72**, 1835 (1998).
[14] S. L. Zang, W. Ding, Y. Yan, J. Qu, B. Li, L. Y. Li, K. T. Yue, and D. P. Yu, Appl. Phys. Lett. **81**, 4446 (2002).
[15] D. P. Yu, Z. G. Bai, Y. Ding, Q. L. Hang, H. Z. Zhang, J. J. Wang, Y. H. Zou, W. Qian, G. C. Xiong, H. T. Zhou, and S. Q. Feng, Appl. Phys. Lett. **72**, 3458 (1998).
[16] R. P. Wang, G. W. Zhou, Y. L. Liu, S. H. Pan, H. Z. Zhang, D. P. Yu, and Z. Zhang, Phys. Rev. B **61**, 16827 (2000).
[17] S. Piscanec, A. C. Ferrari, M. Cantoro, S. Hofmann, J. A. Zapien, Y. Lifshift, S. T. Lee, and J. Robertson, Mater. Sci. Eng., C **23**, 931 (2003).
[18] R. Gupta, Q. Xiong, C. K. Adu, U. J. Kim, and P. C. Eklund, Nano Lett. **3**, 627 (2003).
[19] K. W. Adu, H. R. Gutierrez, U. J. Kim, and P. C. Eklund, Nano Lett. **5**, 409 (2005).
[20] D. Li, Y. Wu, P. Kim, P. Yang, and A. Majumdar, Appl. Phys. Lett. **83**, 2934 (2003).
[21] A. M. Morales and M. C. Lieber, Science **279**, 208 (1998).
[22] K. W. Adu, H. R. Gutierrez, U. J. Kim, and P. C. Eklund (unpublished).
[23] Y. Maeda, Phys. Rev. B **51**, 1658 (1995).
[24] G. Nilsson and G. Nelin, Phys. Rev. B **6**, 3777 (1972).
[25] "This value of $\Gamma=4.7$ cm^{-1} is obtained by fitting the 520 cm^{-1} band for bulk Si under identical micro-Raman optical conditions to those used to obtain the nanowire spectra. This experiment for (bulk Si) was carried out at low laser power."
[26] J. J. Kirkland, W. W. Yau, H. J. Stoklosa, and C. H. Dilks, J. Chromatogr. Sci. **15**, 303 (1977).
[27] J. Raptis, E. Liarokapis, and E. Anastassakis, Appl. Phys. Lett. **44**, 125 (1984).
[28] M. Balkanski, R. F. Wallis, and E. Haro, Phys. Rev. B **28**, 1928 (1983).
[29] J. H. Moore, C. C. Davis, and M. A. Coplan, *Building Scientific Apparatus* (Addison–Wesley, London, 1983), p. 125.